Pro-515 of the dynamin-like GTPase MxB contributes to HIV-1 inhibition by regulating MxB oligomerization and binding to HIV-1 capsid

Received for publication, December 24, 2019, and in revised form, March 24, 2020 Published, Papers in Press, March 26, 2020, DOI 10.1074/jbc.RA119.012439

Fengwen Xu[‡§1], Fei Zhao[‡§1], Xiaoxiao Zhao[‡§], Di Zhang[‡§], Xiaoman Liu[‡§], Siqi Hu[‡§], Shan Mei[‡§], Zhangling Fan[‡§], Yu Huang[‡§], Hong Sun[‡§], Liang Wei[‡§], Chao Wu[‡], Quanjie Li[¶], Jianwei Wang[‡], Shan Cen[¶], Chen Liang[‖], and Fei Guo[‡§2]

From the [‡]NHC Key Laboratory of Systems Biology of Pathogens, Institute of Pathogen Biology, and the [§]Center for AIDS Research, Chinese Academy of Medical Sciences and Peking Union Medical College, Beijing 100730, China, the [¶]Institute of Medicinal Biotechnology, Chinese Academy of Medical Sciences and Peking Union Medical College, Beijing 100050, China, and the [‖]McGill University AIDS Centre, Lady Davis Institute, Jewish General Hospital, Montreal H3T 1E2, Quebec, Canada

Edited by Craig E. Cameron

Interferon-regulated myxovirus resistance protein B (MxB) is an interferon-induced GTPase belonging to the dynamin superfamily. It inhibits infection with a wide range of different viruses, including HIV-1, by impairing viral DNA entry into the nucleus. Unlike the related antiviral GTPase MxA, MxB possesses an N-terminal region that contains a nuclear localization signal and is crucial for inhibiting HIV-1. Because MxB previously has been shown to reside in both the nuclear envelope and the cytoplasm, here we used bioinformatics and biochemical approaches to identify a nuclear export signal (NES) responsible for MxB's cytoplasmic location. Using the online computational tool LocNES (Locating Nuclear Export Signals or NESs), we identified five putative NES candidates in MxB and investigated whether their deletion caused nuclear localization of MxB. Our results revealed that none of the five deletion variants relocates to the nucleus, suggesting that these five predicted NES sequences do not confer NES activity. Interestingly, deletion of one sequence, encompassing amino acids 505–527, abrogated the anti-HIV-1 activity of MxB. Further mutation experiments disclosed that amino acids 515–519, and Pro-515 in particular, regulate MxB oligomerization and its binding to HIV-1 capsid, thereby playing an important role in MxB-mediated restriction of HIV-1 infection. In summary, our results indicate that none of the five predicted NES sequences in MxB appears to be required for its nuclear export. Our findings also reveal several residues in MxB, including Pro-515, critical for its oligomerization and anti-HIV-1 function.

A group of cellular proteins have been discovered to possess potent anti-HIV-1 activity. These include APOBEC3G (apolipoprotein B mRNA-editing catalytic polypeptide 3G) (1), TRIM5α (tripartite motif protein 5-α) (2, 3), ZAP (zinc-finger antiviral protein) (4), tetherin (5, 6), SAMHD1 (SAM domain– and HD domain– containing protein 1) (7–11), IFITM (interferon- induced transmembrane protein) (12–14), MxB (15–17), SERINC5 (serine incorporator 5) (18–20), and others. MxB is one of the interferon-induced myxovirus resistance proteins that restrict a wide range of different viruses. Infection of some RNA and DNA viruses, such as influenza viruses, vesicular stomatitis virus, Thogoto virus, and hepatitis B virus, has been reported to be restricted by human MxA (21–25). The antiviral function of MxB was only reported recently, inhibiting HIV-1, herpesviruses, and hepatitis C virus (15–17, 26–31).

Both MxA and MxB are GTPases, belonging to the dynamin superfamily. They share 63% sequence identity and a similar structure, containing a GTPase domain, bundle signaling elements (BSE)[3] domain, and a stalk domain (32–34). Different from MxA, MxB has an extra N-terminal region, which has a nuclear localization signal (NLS), contributing to binding to HIV-1 capsid, and is indispensable for inhibiting HIV-1 infection (35–38). Several nucleoporins, components of the nuclear pore complex, were recently shown to assist MxB to localize at the nuclear pore complex and facilitate MxB inhibition of HIV-1 (39, 40). In addition to the NLS, MxB oligomerization is also central to inhibit HIV-1 (36, 38, 41–43). The cryo-EM structures of MxB reveal that MxB assembles into helical tubes consisting of MxB dimer units (43). Six dimers interlock with each other to form one rung, and the sixth dimer interacts with the first dimer to help form the helical tube. The crystal and cryo-EM structures of MxB have the dimer interface (interface

This work was supported by National Key Plan for Scientific Research and Development of China Grant 2016YFD0500307; Ministry of Science and Technology of China Grants 2018ZX10301408-003 and 2018ZX10731101-001-018; CAMS Innovation Fund for Medical Sciences (CIFMS) Grants CIFMS 2017-I2M-1-014 and CIFMS 2018-I2M-3-004; National Natural Science Foundation of China Grants 81401673, 81528012, 81601771, 81702451, and 81371808; Canadian Institutes of Health Research Grant CCI-132561; CAMS general fund Grant 2019-RC-HL-012; and PUMC Youth Fund/Fundamental Research Funds for the Central Universities Grants 3332018202 and 3332019157. The authors declare that they have no conflicts of interest with the contents of this article.

[1] Both authors contributed equally to this work.

[2] To whom correspondence should be addressed: MOH Key Laboratory of Systems Biology of Pathogens and Center for AIDS Research, Institute of Pathogen Biology and Center for AIDS Research, Chinese Academy of Medical Sciences and Peking Union Medical College, Beijing 100730, China. Tel.: 86-10-67855028; Fax: 86-10-67855028; E-mail: guofei@ipb.pumc.edu.cn.

[3] The abbreviations used are: BSE, bundle-signaling elements; NLS, nuclear localization signal; NES, nuclear export signal; DSS, disuccinimidyl suberate; VSV-G, vesicular stomatitis virus glycoprotein; DAPI, 4′,6-diamidino-2-phenylindole; IP, immunoprecipitation.

Table 1
The putative NES in MxB
Online software (LocNES) (51) was used to predict the putative NES in MxB. Putative NES with high scores and overlapping sequences are shown.

Position (aa)	Sequence	Score
51–65	GAEKDAAFLAKDFNF	0.254
52–66	AEKDAAFLAKDFNFL	0.483
54–68	KDAAFLAKDFNFLTL	0.764
98–112	RPCIDLIDSLRALGV	0.508
104–118	IDSLRALGVEQDLAL	0.157
109–123	ALGVEQDLALPAIAV	0.099
199–213	GNGRGISHELISLEI	0.077
207–221	ELISLEITSPEVPDL	0.129
209–223	ISLEITSPEVPDLTI	0.078
374–388	LTTELIMHIQKSLPL	0.068
375–389	TTELIMHIQKSLPLL	0.037
505–519	VHQYIQQLVEPALSM	0.272
512–526	LVEPALSMLQKAMEI	0.088
513–527	VEPALSMLQKAMEII	0.286

2), oligomer interfaces (interface 1 and 3), and helical assembly interface (interface 4) (43, 44). Interface 2 mutations M574D, Y651D, and M567D/L570D disrupt MxB dimerization and thus are unable to inhibit HIV-1 (38, 41–44). Mutations F495D and R449D in interface 3 prevent oligomerization and also diminish its anti-HIV-1 activity (43, 44).

In this study, given that MxB is found in both the nuclear envelope and the cytoplasm (36, 38, 44–47), we used online software to predict the putative nuclear export signal (NES) in MxB that might have led to the cytoplasmic location of MxB and further tested their nuclear export functions by deleting each of the five candidates. All of these five deleted MxB mutants were still found in the cytoplasm, suggesting that none of these five sequences bears NES activity. To our surprise, we found that the MxBdel(505–527) mutant lost both its ability to impair HIV-1 infection and the subcellular localization pattern of WT MxB. Further study showed that amino acids 515–519 (especially Pro-515) were critical for oligomerization of MxB and capsid-binding ability and thus essential for MxB antiviral activity.

Results

Deletion of amino acids 505–527 diminishes antiviral ability of MxB

Although it was reported that MxB had an NLS at its N terminus, MxB was found in the cytoplasm (36, 38, 44–47). It is unclear whether MxB has an NES to assist its translocation from nucleus to cytoplasm. Using online software to predict the putative NES in MxB (LocNES) (51), several high-score regions with overlapping sequences were suggested (Table 1). Thus, we created five DNA constructs, each deleting one of these potential regions, named the 51–68, 98–123, 199–223, 374–389, 505–527 deletions. A schematic representation of these five deletions is shown in Fig. 1*A*. These five mutants, WT MxB, or N-terminal (residues 1–25) deletion were transfected into HeLa cells. As shown in Fig. 1*B*, MxB was localized at the nuclear envelope and in the form of cytoplasmic puncta/granules, whereas the N-terminal (residues 1–25) deletion, lacking the NLS, was dispersed in the cytoplasm. All of the five NES deletion candidates were seen in the cytoplasm, suggesting that these five sequences do not bear NES function.

In the meantime, we measured the antiviral activity of these MxB deletions. Cells were transfected with these DNA constructs and then infected with vesicular stomatitis virus glycoprotein (VSV-G) pseudotyped HIV-$1_{NL4-3-\Delta E-YFP}$. Infected cells were scored by flow cytometry. The results showed that the MxBdel(505–527) mutant exhibited dramatically decreased antiviral activity, similar to the MxBdel(1–25) mutant (Fig. 1*C*, *top*). The expression levels of these deletions were comparable with WT MxB (Fig. 1*C*, *bottom*). Previous reports showed that the stalk domain of MxB contains leucine zipper repeats, contributes to MxB dimerization, and is critical for restricting HIV-1 (36, 38, 41, 42, 45). To test whether the loss of antiviral activity of MxBdel(505–527) was due to the lack of dimer formation, the WT or MxB mutants tagged with a FLAG epitope were tested for association with Myc-MxB by immunoprecipitation. Only the dimer interface mutant 574/651D lost the ability to oligomerize, and the five deletions did not disrupt MxB homodimer formation (Fig. 1*D*).

Deletion of amino acids 515–519 impairs the antiviral ability of MxB

To determine which amino acids in the region of 505–527 are required for the anti-HIV-1 activity of MxB, we used alanine to replace every five amino acids and generated mutants (505–509)A, (510–514)A, (515–519)A, (520–524)A, and (525–527)A (Fig. 2*A*). Subcellular localization of these MxB mutants was analyzed by indirect immunofluorescence microscopy. As shown in Fig. 2*B*, mutants (505–509)A, (510–514)A, (520–524)A, (525–527)A, and WT MxB all accumulated at the nuclear envelope with large cytoplasmic puncta/granules, whereas (515–519)A exhibited dispersed distribution in the cytoplasm. Then cells were transfected with WT or these mutated MxB DNA and infected with VSV-G pseudotyped HIV-$1_{NL4-3-\Delta E-YFP}$. Mutants (505–509)A, (510–514)A, (520–524)A, and (525–527)A showed anti-HIV-1 activity similar to WT MxB, whereas MxB(515–519)A was as impaired as MxBdel(1–25) and MxBdel(505–527) in inhibiting HIV-1 (Fig. 2*C*, *top*). Expression levels of these mutations were comparable with WT MxB (Fig. 2*C*, *bottom*). Results of co-immunoprecipitation assays showed that all MxB mutants, including (515–519)A, interacted with Myc-MxB as efficiently as the WT except MxB574/651D (Fig. 2*D*), which suggests that MxB(515–519)A is able to form a homodimer yet is defective in inhibiting HIV-1.

Pro-515 is important for the antiviral activity of MxB

To understand the role of the individual amino acids within region 515–519 in MxB inhibiting HIV-1, we mutated each amino acid to alanine (Fig. 3*A*). Results of immunofluorescence experiments showed that mutants MxB515A, MxB517A, MxB518A, and MxB519A exhibited similar patterns of distribution at the nuclear envelope with cytoplasmic puncta (Fig. 3*B*). These MxB mutant–expressing HEK293 cells were infected with VSV-G pseudotyped HIV-$1_{NL4-3-\Delta E-YFP}$. Results of flow cytometry showed that the antiviral activity of MxB decreased when Pro-515 was mutated, whereas its expression levels were similar to that of MxB (Fig. 3*C*). Co-immunoprecipitation assays showed that MxB mutants MxB515A, MxB517A, MxB518A, and MxB519A interacted with Myc-

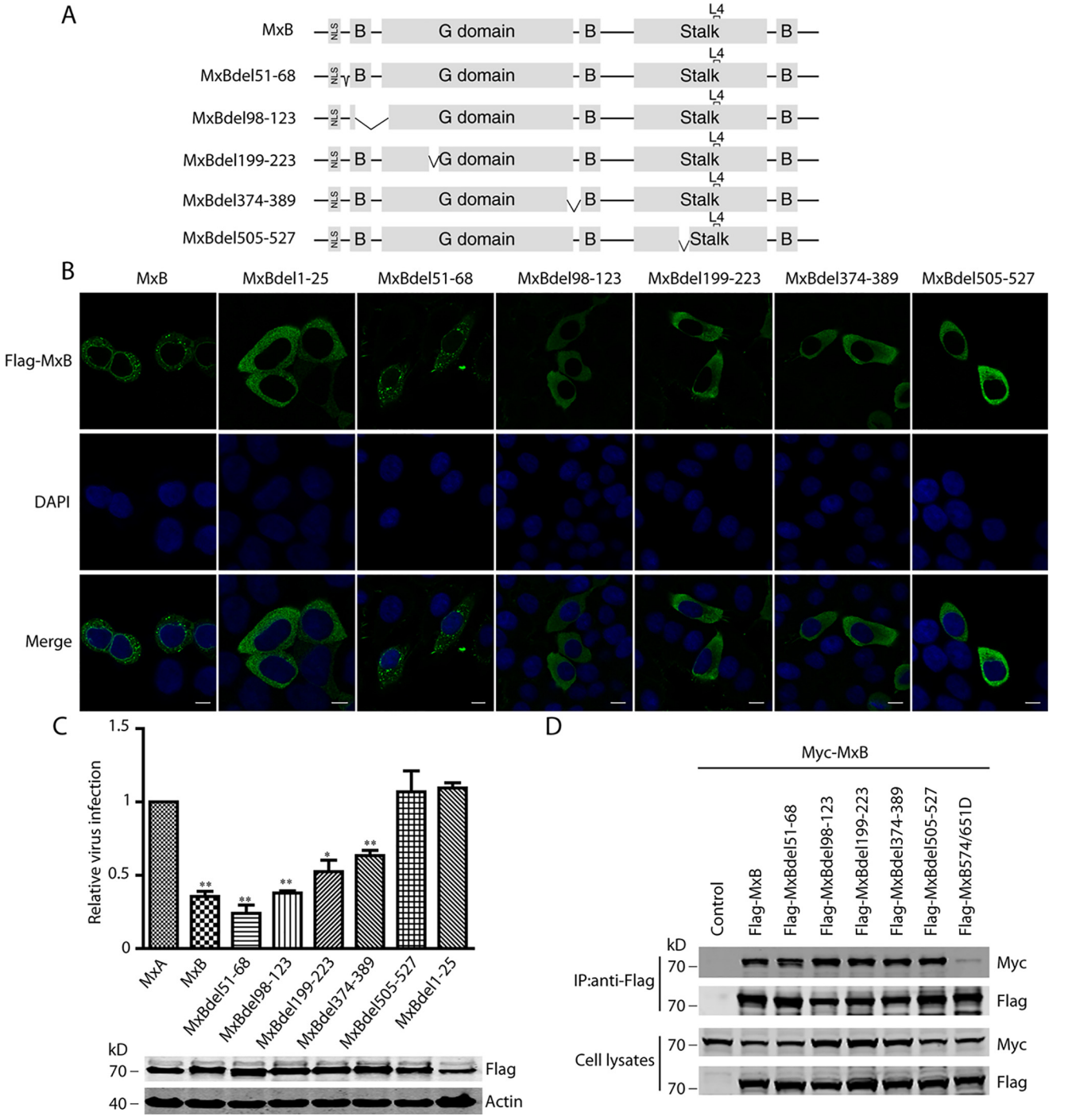

Figure 1. Deletion of amino acids 505–527 impairs the anti-HIV-1 activity of MxB. *A*, *schematic representation* of putative NES deletions. *B*, indirect immunofluorescence analysis of HeLa cells that were transfected with WT MxB DNA or truncations (anti-FLAG; *green*). The nuclei were stained with DAPI (*blue*). *Scale bar*, 10 μm. *C*, cells were transfected with WT MxB DNA or truncations and then infected with VSV-G pseudotyped HIV-$1_{NL4-3-\Delta E-YFP}$ for 48 h. Flow cytometry was performed to measure HIV-1 infection. Cells expressing MxA were challenged with HIV-$1_{NL4-3-\Delta E-YFP}$ as a control. *Error bars*, S.D. (***, $p < 0.001$; **, $p < 0.01$; *, $p < 0.05$, *t* test). The expression of MxA, MxB, and truncations is shown in at the *bottom*. *D*, co-immunoprecipitation of FLAG-tagged WT MxB or truncations together with Myc-MxB. HEK293T cells were transfected with plasmids expressing Myc-tagged MxB together with FLAG-MxB or truncations. FLAG-tagged proteins were immunoprecipitated with anti-FLAG antibody, followed by Western blotting with the indicated antibodies.

MxB as efficiently as the WT (Fig. 3*D*), which suggests that these mutants did not disrupt MxB homodimer formation.

Mutations (515–519)A and MxB515A inhibit the formation of oligomer

The three-dimensional density map (Protein Data Bank ID 5UOT) of the MxB helical assembly has been determined by Alvarez *et al.* (43) at 4.6 Å resolution, through cryo-EM and real-space helical reconstruction. MxB was shown to assemble into highly ordered long helical tubes like other dynamin family members. Oligomerization of MxB has been shown to be essential for binding to HIV-1 core and inhibiting HIV-1 infection (36, 38, 41–43). The cryo-EM structure of the MxB assembly reveals that amino acids 515–519 are located on the Sα2 helix of

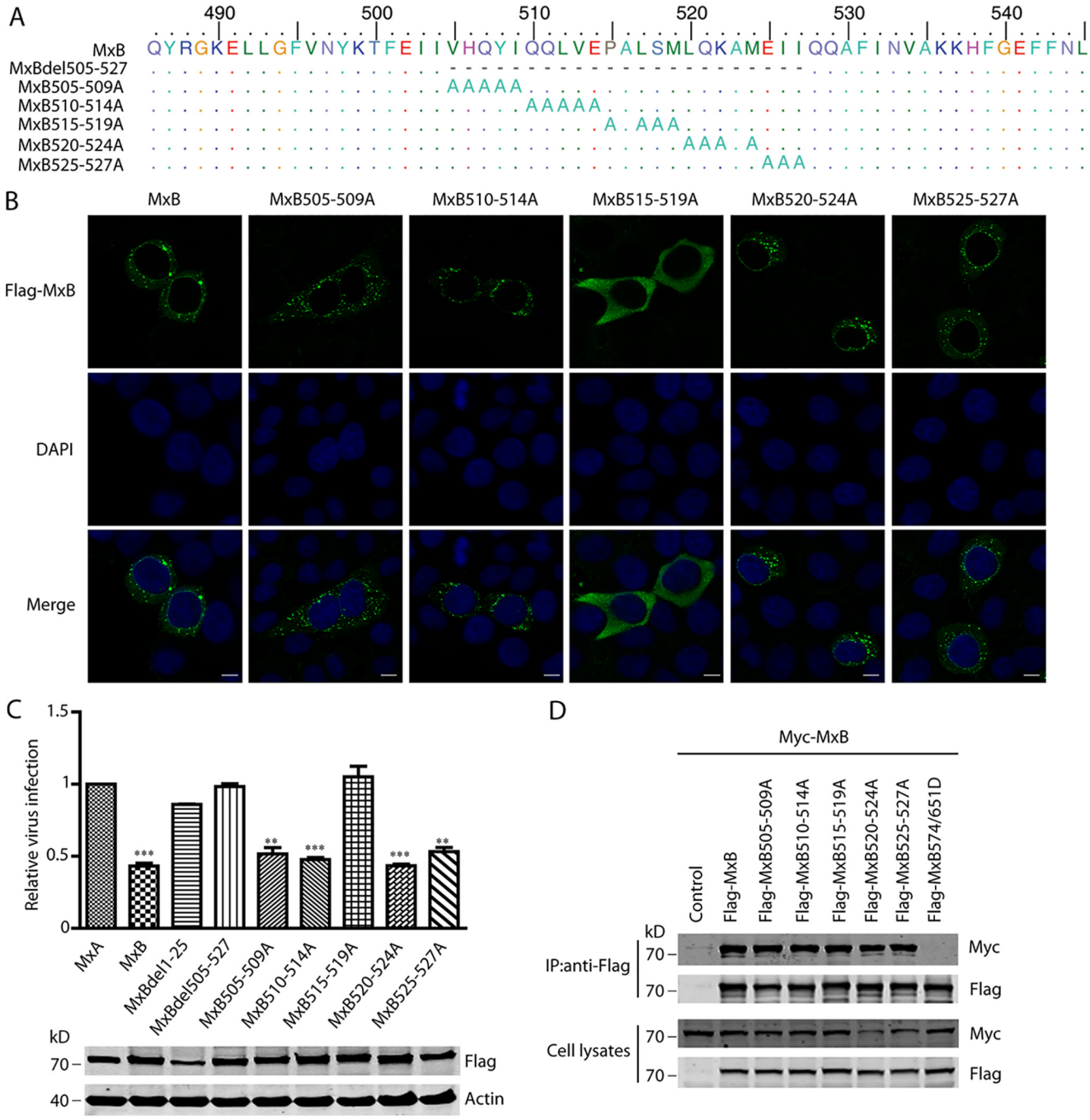

Figure 2. The (515–519)A mutation loses the ability to inhibit HIV-1. *A*, *schematic representation* of the substitution mutations. *B*, indirect immunofluorescence analysis of HeLa cells transfected with WT or mutated MxB DNA (anti-FLAG; *green*). The nuclei were stained with DAPI (*blue*). *Scale bar*, 10 μm. *C*, cells were transfected with WT or mutated MxB DNA and then infected with VSV-G pseudotyped HIV-$1_{NL4-3-\Delta E-YFP}$ for 48 h. Flow cytometry was performed to score HIV-1–infected cells. Cells expressing MxA were infected with HIV-$1_{NL4-3-\Delta E-YFP}$ as a control. *Error bars*, S.D. (***, $p < 0.001$; **, $p < 0.01$; *, $p < 0.05$, *t* test). The expression of MxA, MxB, and mutants is shown at the *bottom*. *D*, co-immunoprecipitation of FLAG-tagged WT MxB or mutants together with Myc-MxB. HEK293T cells were transfected with plasmids expressing Myc-tagged MxB together with FLAG-MxB or mutants. FLAG-tagged proteins were immunoprecipitated with anti-FLAG antibody, followed by Western blotting with the indicated antibodies.

MxB, which is adjacent to oligomer interface 3 (Fig. 4, *A* and *B*). It was reported that interface 3 mutations (R449D and F495D) abrogate MxB oligomerization and diminish its anti-HIV-1 activity (43), which suggests that mutating the sequence of 515–519 may affect the hydrophobic interactions at interface 3 and thus alter rung stacking and oligomer formation. We therefore measured the antiviral activity of interface 2 mutant (MxB574/651D) and interface 3 mutant (MxB449/495D), together with MxB(515–519)A and MxB515A. As shown in Fig. 4*C*, interface 2 mutant (MxB574/651D) and interface 3 mutant (MxB449/495D) lost their antiviral activity, consistent with previous reports (36, 38, 41–44). MxB(515–519)A and MxB515A were as impaired as MxB449/495D in inhibition of HIV-1.

To determine the oligomerization ability of MxB(515–519)A and MxB515A, a chemical cross-linking assay and gel filtration

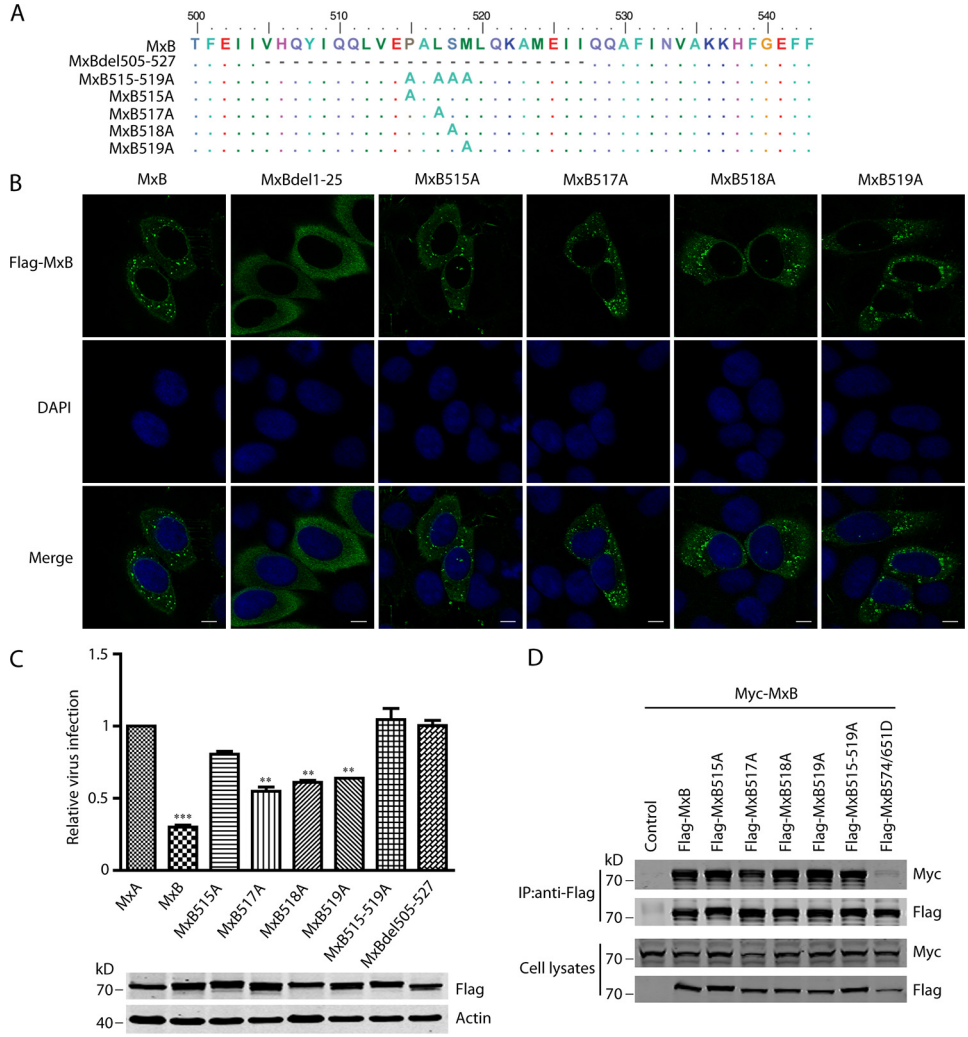

Figure 3. Mutation of Pro-515 decreases MxB anti-HIV-1 activity. *A*, *schematic representation* of substitution mutations. *B*, indirect immunofluorescence analysis of HeLa cells transfected with WT or mutated MxB DNA (anti-FLAG; *green*). The nuclei were stained with DAPI (*blue*). *Scale bar*, 10 μm. *C*, HEK293 cells expressing WT or mutated MxB were infected with VSV-G pseudotyped HIV-$1_{NL4-3-\Delta E-YFP}$ for 48 h. Flow cytometry was performed to measure HIV-1 infection efficiency. Cells expressing MxA were challenged with VSV-G pseudotyped HIV-$1_{NL4-3-\Delta E-YFP}$ as a control. *Error bars*, S.D. (***, $p < 0.001$; **, $p < 0.01$; *, $p < 0.05$, *t* test). The expression of MxA, MxB, and mutants is shown at the *bottom*. *D*, co-immunoprecipitation of FLAG-tagged WT MxB or mutants together with Myc-MxB. HEK293T cells were transfected with plasmids expressing Myc-tagged MxB together with FLAG-MxB or mutants. FLAG-tagged proteins were immunoprecipitated with anti-FLAG antibody, followed by Western blotting with the indicated antibodies.

chromatography were performed. As determined by cross-linking with disuccinimidyl suberate (DSS), the interface 2 mutant MxB574/651D lost its oligomerization ability completely (Fig. 5*A*). Similar to interface 3 mutant MxB449/495D, MxB(515–519)A was defective in oligomer formation, and oligomerization of MxB515A decreased as well. Furthermore, the results of gel filtration chromatography showed that the higher-molecular weight oligomerization of MxB449/495D, MxB574/651D, MxB(515–519)A, and MxB515A decreased with concomitant increase in lower-molecular-mass complexes (Fig. 5*B*), which correlates with their incapability to inhibit HIV-1 infection. These data suggest that loss of oligomerization has led to the deficiency of MxB(515–519)A and MxB515A in inhibiting HIV-1.

The 515–519A and 515A mutants lose the ability to bind HIV-1 capsid

It was previously reported that MxB dimerization and binding to HIV-1 capsid are necessary for inhibiting HIV-1 infection (36, 38, 41–44). To measure the binding of (515–519)A to HIV-1 capsid, we performed step gradient analyses to detect the interaction between p24 and MxB (WT, MxB449/495D, and MxB(515–519)A). WT MxB showed strong interaction with p24. Interface 3 mutant MxB449/495D reduced MxB binding to HIV-1 capsid, and the capsid binding ability of (515–519)A was also dramatically reduced (Fig. 6, *A–C*). These data suggest that the lack of binding to HIV-1 capsid underlies the loss of HIV-1 inhibition by (515–519)A. Association of 515A mutant with HIV-1 capsid was also disrupted, as opposed to moderate or no adverse effect by the other mutants, MxB517A, MxB518A, and MxB519A (Fig. 6, *D* and *E*).

Discussion

The N-terminal 25 amino acids are essential for the anti-HIV-1 activity of MxB by regulating MxB subcellular localization and binding to HIV-1 capsid (15–17, 35, 36, 38, 45, 46). The amino acids ^{11}RRR^{13} are involved in association with HIV-1 capsid; mutation of ^{11}RRR^{13} impairs the anti-HIV-1 function

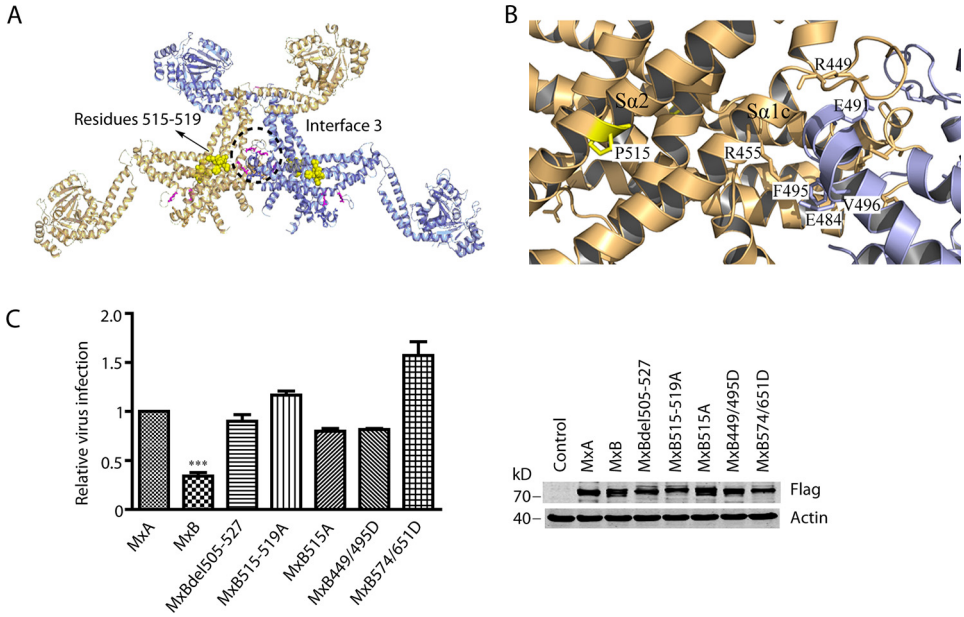

Figure 4. Amino acids 515–519 close to interface 3 affect MxB oligomerization. *A*, the cryo-EM structure of an MxB oligomer reveals that amino residues 515–519 (*yellow*) are located on the Sα2 helix, which is adjacent to interface 3 (*magenta* and *black circle*). *B*, *expanded views* of interface 3. *C*, cells expressing WT or mutated MxB were infected with VSV-G pseudotyped HIV-$1_{NL4-3-\Delta E-YFP}$ for 48 h. Flow cytometry was performed to measure HIV-1 infection efficiency. Cells expressing MxA were challenged with VSV-G pseudotyped HIV-$1_{NL4-3-\Delta E-YFP}$ as a control. *Error bars*, S.D. (***, $p < 0.001$; **, $p < 0.01$; *, $p < 0.05$, *t* test). The expression of MxA, MxB, and mutants is shown on the *right*.

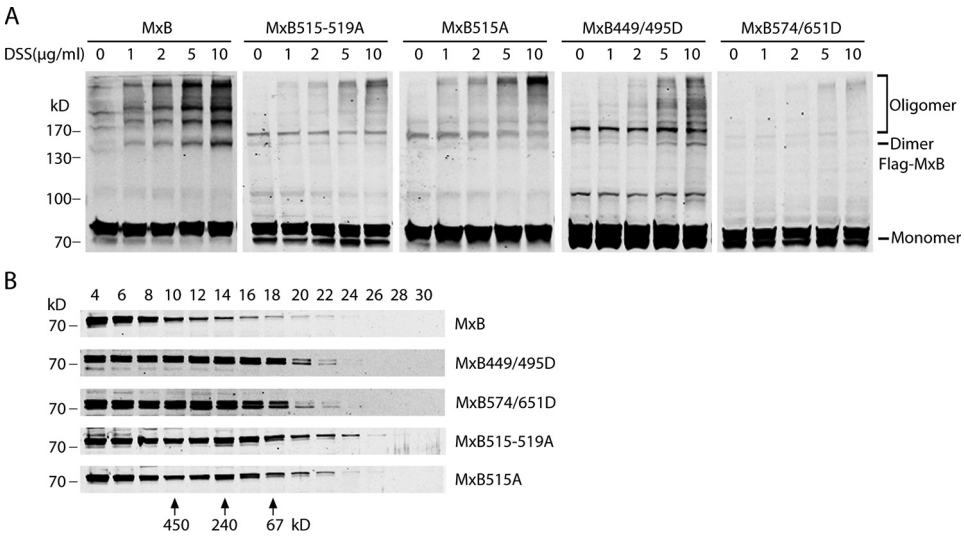

Figure 5. MxB(515–519)A and MxB515A are defective in oligomerization. *A*, cells expressing FLAG-tagged WT MxB or MxB mutants (MxB449/495D, MxB574/651D, MxB515–519A, or MxB515A) were harvested and lysed. DSS was then added into lysates at an increasing concentration of 0–10 μg/ml (0 indicates DMSO only). After 1 h, the reaction was quenched, and FLAG-tagged protein was resolved by 6% SDS-PAGE and detected by Western blotting. *B*, cell lysates expressing WT or mutated MxB were fractionated on a Superdex 200 gel filtration column. Different fractions were analyzed by Western blotting.

(35, 36). Amino acids ^{20}KY^{21} contribute to the NLS function, yet mutation of Lys^{20} does not affect MxB inhibition of HIV-1 infection, casting doubt on the role of NLS in MxB anti-HIV-1 activity (35). Because MxB is localized to both the nucleus and the cytoplasm (36, 38, 44–47), it is speculated that MxB has a NES to assist its translocation. In this study, using online software to predict the putative NES of MxB, we identified five regions and deleted each of these five sequences to test their potential NES function. Unfortunately, these five sequences do not bear NES function.

MxB mutants del(98–123), del(199–223), del(374–389), del(505–527), and (515–519)A showed dispersed distribution in the cytoplasm, yet del(98–123), del(199–223), and del(374–389) preserved certain levels of anti-HIV-1 activity. This may reflect the possibility that these MxB mutants retain the ability of binding HIV-1 capsid, thus inhibiting HIV-1 infection. However, the del(505–527), (515–519)A, and 515A mutations abrogate the ability to inhibit HIV-1. Different from del(505–527) and (515–519)A, the 515A single mutation still exhibits punctate cytoplasmic distribution. Future study is needed to determine whether the punctate localization of MxB is important for the antiviral function.

MxB is able to assemble into highly ordered helical tubes. Using molecular dynamics flexible fitting, the cryo-EM struc-

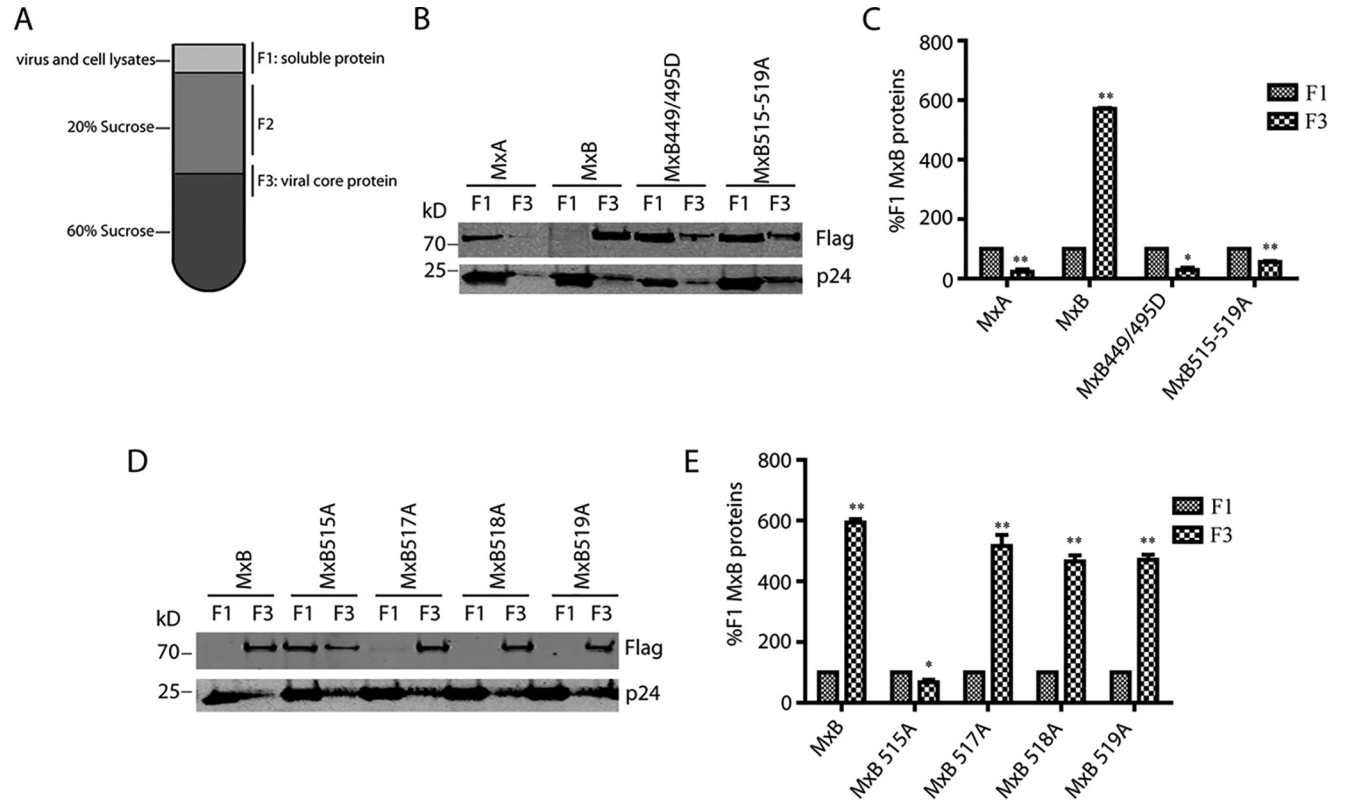

Figure 6. MxB mutants (515–519)A and 515A are deficient in binding to HIV-1 capsid. *A*, illustration of MxB-HIV-1 capsid-binding assay. VSV-G pseudotyped HIV-$1_{NL4-3-\Delta E\text{-}YFP}$ viruses were mixed with MxB (WT or mutants) containing cell lysates, treated with 0.1% Triton X-100, and loaded onto step sucrose gradients. *B* and *D*, the individual gradient fractions representing soluble MxB (*F1*) and core-associated MxB (*F3*) were subjected to immunoblot analysis. Antibody against HIV-1 CAp24 was used as control. *C* and *E*, intensity of FLAG-tagged protein band was quantified using ImageJ (National Institutes of Health). *Error bars*, S.D. (***, $p < 0.001$; **, $p < 0.01$; *, $p < 0.05$, *t* test).

ture of MxB assembly reveals that six MxB dimers are interconnected one by one to form a rung, which further forms a one-start helical tube (43). The ability to dimerize has been shown to be critical for its antiviral activity, as the dimer interface mutations ablate the ability to inhibit HIV-1 (36, 38, 41–44). Mutations (F495D, R449D, and E484K) in one of the oligomerization interfaces, interface 3, lose both the ability to form oligomers and the ability to restrict HIV-1 (43). Here we observed that the (515–519)A mutation disrupts the anti-HIV-1 activity of MxB. Based on the cryo-EM structure, amino acids 515–519 are located adjacent to oligomer interface 3. The (515–519)A and 515A mutations may thus affect the hydrophobic interactions at interface 3 and affect rung stacking and oligomer formation. Indeed, results of chemical cross-linking and gel filtration chromatography showed that (515–519)A and 515A mutations diminish MxB oligomerization. We have also tested the capsid binding ability of these mutations and observed that (515–519)A and 515A did not bind to HIV-1 capsid. This indicates possible association between MxB oligomerization and its binding to HIV-1 capsid. Oligomerization of MxB has been reported to play a pivotal role in inhibiting HIV-1 and herpesviruses, likely through a coordinated binding to viral capsid and thus blockade of viral DNA from entering the nucleus (26–28, 36, 38, 41–44). Through investigating a series of MxB mutants, we have identified new amino acids in MxB, including amino acids 515–519, which participate in MxB oligomerization and contribute to the antiviral function of MxB. Our data further strengthen the importance of MxB oligomerization in viral restriction.

Experimental procedures

Plasmids and cells

The FLAG-tagged MxB in the pQCXIP expression vector was described previously (15). The Myc-tagged MxB, MxB deletions, and mutations were generated with PCR or the KOD-Plus mutagenesis kit (TOYOBO). Plasmid DNA was transfected into cells using polyethyleneimine (Sigma–Aldrich) in accordance with the manufacturer's instructions. HEK293T cells, HeLa cells, and HEK293 cells were cultured in Dulbecco's modified Eagle's medium containing 10% fetal bovine serum (Gibco), 1% penicillin and streptomycin (100×; Solarbio). HEK293 cells stably expressing MxB were constructed by pQCXIP plasmids expressing WT or mutant MxB proteins transfection and puromycin (0.6 μg/ml) selection.

HIV-1 pseudovirus stock preparation and infection

VSV-G pseudotyped HIV-$1_{NL4-3-\Delta E\text{-}YFP}$ was prepared by transfecting HEK293T cells with HIV-$1_{NL4-3-\Delta E\text{-}YFP}$ DNA and VSV-G DNA. The pseudoviruses in supernatants were harvested at 48 h after transfection. MxA- or MxB-transfected HEK293T cells were incubated with VSV-G pseudotyped HIV-$1_{NL4-3-\Delta E\text{-}YFP}$ for 48 h. Cells were harvested and fixed in 1% paraformaldehyde, permeabilized by 0.1% Triton X-100 for 10 min, and then stained with Alexa Fluor® 647–conjugated

FLAG antibody (Cell Signaling Biotechnology). Flow cytometry was used to quantitate the infection of HIV-1.

Western blotting

Cells were lysed in radioimmune precipitation assay buffer comprised of 25 mM Tris/HCl (pH 7.4), 150 mM NaCl, 1% Nonidet P-40, 0.25% sodium deoxycholate, 1 mM EDTA, and a proteinase inhibitor mixture (Sigma–Aldrich). Lysates were cleared by centrifugation. Proteins were separated by SDS-PAGE and then transferred onto the nitrocellulose membranes (Millipore). After blocking in 5% (w/v) nonfat skim milk for 1 h, membranes were incubated with anti-FLAG antibody (Sigma–Aldrich), anti-Myc antibody (Sigma–Aldrich), anti-actin antibody (Sigma–Aldrich), or anti-p24 antibody (Sino Biological) at 4 °C for overnight. The corresponding IRDye™ secondary antibodies (Odyssey) were then applied to the membranes. After extensive washing, the membranes were scanned by the Odyssey IR imaging system (LI-COR). Protein signals were quantified using the ImageJ automated digitizing program (National Institutes of Health).

Immunoprecipitation assay

Immunoprecipitation was conducted as described previously (48). Briefly, cells were lysed in radioimmune precipitation assay buffer 48 h post-transfection. After centrifugation, cell lysates were incubated with anti-FLAG antibody–conjugated agarose (Sigma–Aldrich) at 4 °C for overnight. After extensive washing, agarose was boiled in SDS-PAGE sample buffer. Then Western blotting was performed as described above.

Immunofluorescence staining and confocal microscopy

For immunostaining, transfected HeLa cells were fixed in 4% paraformaldehyde for 10 min and then permeabilized by 0.1% Triton X-100 for 10 min. After incubation in blocking buffer, staining was performed with anti-FLAG antibody (Sigma–Aldrich) for 1 h, followed by anti-mouse Alexa Fluor® 488–conjugated antibody (Thermo Scientific) incubation. DAPI was used for nuclei staining. Images were acquired with a Leica TCS SP5, DMI6000 confocal microscope (Leica Microsystems).

Cross-linking assay

As described previously (42), FLAG-tagged MxB or mutants transfected HEK293T cells were harvested and lysed with 0.5% Nonidet P-40/PBS. Cell lysates were cleared by centrifugation at 16,000 × *g* for 10 min. Supernatants were incubated with DSS (Thermo Scientific) at different final concentrations for 1 h at room temperature. The mixtures were then incubated with SDS-PAGE sample buffer for 30 min at 37 °C. Samples were resolved by 6% SDS-PAGE and detected by Western blotting.

Gel filtration chromatography

For gel filtration chromatography, 1×10^7 HEK293T cells expressing MxB or mutants were collected and lysed in buffer containing 20 mM Tris/HCl (pH 7.4), 150 mM NaCl, and 14 mM CHAPS. Cell lysates were separated using a Superdex™ 200 column (GE Healthcare) at an elution rate of 0.5 ml/min. Samples from each fraction were analyzed by Western blotting.

Step gradient analyses

1×10^7 HEK293T cells expressing MxB or mutants were lysed in buffer comprised of 10 mM Tris/HCl (pH 7.4), 10 mM KCl, 1.5 mM $MgCl_2$, and 0.5 mM DTT. Purified virus treated with 0.1% Triton X-100 and cell lysates underwent step sucrose gradient analyses as reported (49, 50). The soluble protein–containing fraction (F1) and virus core–containing fraction (F3) were analyzed by Western blotting as described above.

Data availability

All data are contained within the article.

Author contributions—F. X., X. Z., and D. Z. formal analysis; F. X., F. Z., X. Z., and D. Z. investigation; F. X., F. Z., X. Z., D. Z., X. L., S. H., S. M., Z. F., Y. H., H. S., L. W., C. W., and Q. L. methodology; F. X. writing-original draft; F. Z., C. W., Q. L., and S. C. software; F. Z. validation; S. H., J. W., C. L., and F. G. funding acquisition; S. M., S. C., C. L., and F. G. project administration; Y. H., C. W., Q. L., and S. C. resources; C. L. and F. G. supervision; C. L. and F. G. writing-review and editing; F. G. conceptualization.

Acknowledgments—We thank Dr. Jian Li for the valuable discussions and Conghui Wang for technical assistance in performing flow cytometry.

References

1. Sheehy, A. M., Gaddis, N. C., Choi, J. D., and Malim, M. H. (2002) Isolation of a human gene that inhibits HIV-1 infection and is suppressed by the viral Vif protein. *Nature* **418,** 646–650 CrossRef Medline
2. Stremlau, M., Perron, M., Lee, M., Li, Y., Song, B., Javanbakht, H., Diaz-Griffero, F., Anderson, D. J., Sundquist, W. I., and Sodroski, J. (2006) Specific recognition and accelerated uncoating of retroviral capsids by the TRIM5α restriction factor. *Proc. Natl. Acad. Sci. U.S.A.* **103,** 5514–5519 CrossRef Medline
3. Huthoff, H., and Towers, G. J. (2008) Restriction of retroviral replication by APOBEC3G/F and TRIM5α. *Trends Microbiol.* **16,** 612–619 CrossRef Medline
4. Zhu, Y., Chen, G., Lv, F., Wang, X., Ji, X., Xu, Y., Sun, J., Wu, L., Zheng, Y. T., and Gao, G. (2011) Zinc-finger antiviral protein inhibits HIV-1 infection by selectively targeting multiply spliced viral mRNAs for degradation. *Proc. Natl. Acad. Sci. U.S.A.* **108,** 15834–15839 CrossRef Medline
5. Neil, S. J., Zang, T., and Bieniasz, P. D. (2008) Tetherin inhibits retrovirus release and is antagonized by HIV-1 Vpu. *Nature* **451,** 425–430 CrossRef Medline
6. Van Damme, N., Goff, D., Katsura, C., Jorgenson, R. L., Mitchell, R., Johnson, M. C., Stephens, E. B., and Guatelli, J. (2008) The interferon-induced protein BST-2 restricts HIV-1 release and is downregulated from the cell surface by the viral Vpu protein. *Cell Host Microbe* **3,** 245–252 CrossRef Medline
7. Laguette, N., Sobhian, B., Casartelli, N., Ringeard, M., Chable-Bessia, C., Ségéral, E., Yatim, A., Emiliani, S., Schwartz, O., and Benkirane, M. (2011) SAMHD1 is the dendritic- and myeloid-cell-specific HIV-1 restriction factor counteracted by Vpx. *Nature* **474,** 654–657 CrossRef Medline
8. Hrecka, K., Hao, C., Gierszewska, M., Swanson, S. K., Kesik-Brodacka, M., Srivastava, S., Florens, L., Washburn, M. P., and Skowronski, J. (2011) Vpx relieves inhibition of HIV-1 infection of macrophages mediated by the SAMHD1 protein. *Nature* **474,** 658–661 CrossRef Medline
9. Goldstone, D. C., Ennis-Adeniran, V., Hedden, J. J., Groom, H. C., Rice, G. I., Christodoulou, E., Walker, P. A., Kelly, G., Haire, L. F., Yap, M. W., de Carvalho, L. P., Stoye, J. P., Crow, Y. J., Taylor, I. A., and Webb, M. (2011) HIV-1 restriction factor SAMHD1 is a deoxynucleoside triphosphate triphosphohydrolase. *Nature* **480,** 379–382 CrossRef Medline
10. Lahouassa, H., Daddacha, W., Hofmann, H., Ayinde, D., Logue, E. C., Dragin, L., Bloch, N., Maudet, C., Bertrand, M., Gramberg, T., Pancino, G.,

Priet, S., Canard, B., Laguette, N., Benkirane, M., *et al.* (2012) SAMHD1 restricts the replication of human immunodeficiency virus type 1 by depleting the intracellular pool of deoxynucleoside triphosphates. *Nat. Immunol.* **13,** 223–228 CrossRef Medline

11. Baldauf, H. M., Pan, X., Erikson, E., Schmidt, S., Daddacha, W., Burggraf, M., Schenkova, K., Ambiel, I., Wabnitz, G., Gramberg, T., Panitz, S., Flory, E., Landau, N. R., Sertel, S., Rutsch, F., *et al.* (2012) SAMHD1 restricts HIV-1 infection in resting $CD4^+$ T cells. *Nat. Med.* **18,** 1682–1687 CrossRef Medline
12. Brass, A. L., Huang, I. C., Benita, Y., John, S. P., Krishnan, M. N., Feeley, E. M., Ryan, B. J., Weyer, J. L., van der Weyden, L., Fikrig, E., Adams, D. J., Xavier, R. J., Farzan, M., and Elledge, S. J. (2009) The IFITM proteins mediate cellular resistance to influenza A H1N1 virus, West Nile virus, and dengue virus. *Cell* **139,** 1243–1254 CrossRef Medline
13. Lu, J., Pan, Q., Rong, L., He, W., Liu, S. L., and Liang, C. (2011) The IFITM proteins inhibit HIV-1 infection. *J. Virol.* **85,** 2126–2137 CrossRef Medline
14. Huang, I. C., Bailey, C. C., Weyer, J. L., Radoshitzky, S. R., Becker, M. M., Chiang, J. J., Brass, A. L., Ahmed, A. A., Chi, X., Dong, L., Longobardi, L. E., Boltz, D., Kuhn, J. H., Elledge, S. J., Bavari, S., *et al.* (2011) Distinct patterns of IFITM-mediated restriction of filoviruses, SARS coronavirus, and influenza A virus. *PLoS Pathog.* **7,** e1001258 CrossRef Medline
15. Liu, Z., Pan, Q., Ding, S., Qian, J., Xu, F., Zhou, J., Cen, S., Guo, F., and Liang, C. (2013) The interferon-inducible MxB protein inhibits HIV-1 infection. *Cell Host Microbe* **14,** 398–410 CrossRef Medline
16. Kane, M., Yadav, S. S., Bitzegeio, J., Kutluay, S. B., Zang, T., Wilson, S. J., Schoggins, J. W., Rice, C. M., Yamashita, M., Hatziioannou, T., and Bieniasz, P. D. (2013) MX2 is an interferon-induced inhibitor of HIV-1 infection. *Nature* **502,** 563–566 CrossRef Medline
17. Goujon, C., Moncorgé, O., Bauby, H., Doyle, T., Ward, C. C., Schaller, T., Hué, S., Barclay, W. S., Schulz, R., and Malim, M. H. (2013) Human MX2 is an interferon-induced post-entry inhibitor of HIV-1 infection. *Nature* **502,** 559–562 CrossRef Medline
18. Usami, Y., Wu, Y., and Göttlinger, H. G. (2015) SERINC3 and SERINC5 restrict HIV-1 infectivity and are counteracted by Nef. *Nature* **526,** 218–223 CrossRef Medline
19. Rosa, A., Chande, A., Ziglio, S., De Sanctis, V., Bertorelli, R., Goh, S. L., McCauley, S. M., Nowosielska, A., Antonarakis, S. E., Luban, J., Santoni, F. A., and Pizzato, M. (2015) HIV-1 Nef promotes infection by excluding SERINC5 from virion incorporation. *Nature* **526,** 212–217 CrossRef Medline
20. Fackler, O. T. (2015) Spotlight on HIV-1 Nef: SERINC3 and SERINC5 identified as restriction factors antagonized by the pathogenesis factor. *Viruses* **7,** 6730–6738 CrossRef Medline
21. Van Hoeven, N., Belser, J. A., Szretter, K. J., Zeng, H., Staeheli, P., Swayne, D. E., Katz, J. M., and Tumpey, T. M. (2009) Pathogenesis of 1918 pandemic and H5N1 influenza virus infections in a guinea pig model: antiviral potential of exogenous α interferon to reduce virus shedding. *J. Virol.* **83,** 2851–2861 CrossRef Medline
22. Haller, O., Staeheli, P., and Kochs, G. (2009) Protective role of interferon-induced Mx GTPases against influenza viruses. *Rev. Sci. Tech.* **28,** 219–231 CrossRef Medline
23. Reichelt, M., Stertz, S., Krijnse-Locker, J., Haller, O., and Kochs, G. (2004) Missorting of LaCrosse virus nucleocapsid protein by the interferon-induced MxA GTPase involves smooth ER membranes. *Traffic* **5,** 772–784 CrossRef Medline
24. Peltekian, C., Gordien, E., Garreau, F., Meas-Yedid, V., Soussan, P., Willams, V., Chaix, M. L., Olivo-Marin, J. C., Bréchot, C., and Kremsdorf, D. (2005) Human MxA protein participates to the interferon-related inhibition of hepatitis B virus replication in female transgenic mice. *J. Hepatol.* **43,** 965–972 CrossRef Medline
25. Haller, O., and Kochs, G. (2011) Human MxA protein: an interferon-induced dynamin-like GTPase with broad antiviral activity. *J. Interferon Cytokine Res.* **31,** 79–87 CrossRef Medline
26. Crameri, M., Bauer, M., Caduff, N., Walker, R., Steiner, F., Franzoso, F. D., Gujer, C., Boucke, K., Kucera, T., Zbinden, A., Münz, C., Fraefel, C., Greber, U. F., and Pavlovic, J. (2018) MxB is an interferon-induced restriction factor of human herpesviruses. *Nat. Commun.* **9,** 1980 CrossRef Medline
27. Schilling, M., Bulli, L., Weigang, S., Graf, L., Naumann, S., Patzina, C., Wagner, V., Bauersfeld, L., Goujon, C., Hengel, H., Halenius, A., Ruzsics, Z., Schaller, T., and Kochs, G. (2018) Human MxB protein is a pan-herpesvirus restriction factor. *J. Virol.* **92,** e01056-18 CrossRef Medline
28. Staeheli, P., and Haller, O. (2018) Human MX2/MxB: a potent interferon-induced postentry inhibitor of herpesviruses and HIV-1. *J. Virol.* **92,** e00709-18 CrossRef Medline
29. Yi, D. R., An, N., Liu, Z. L., Xu, F. W., Raniga, K., Li, Q. J., Zhou, R., Wang, J., Zhang, Y. X., Zhou, J. M., Zhang, L. L., An, J., Qin, C. F., Guo, F., Li, X. Y., *et al.* (2019) Human MxB inhibits the replication of hepatitis C virus. *J. Virol.* **93,** e01285-18 CrossRef Medline
30. Schoggins, J. W., Wilson, S. J., Panis, M., Murphy, M. Y., Jones, C. T., Bieniasz, P., and Rice, C. M. (2011) A diverse range of gene products are effectors of the type I interferon antiviral response. *Nature* **472,** 481–485 CrossRef Medline
31. Liu, S. Y., Sanchez, D. J., Aliyari, R., Lu, S., and Cheng, G. (2012) Systematic identification of type I and type II interferon-induced antiviral factors. *Proc. Natl. Acad. Sci. U.S.A.* **109,** 4239–4244 CrossRef Medline
32. Haller, O., and Kochs, G. (2002) Interferon-induced mx proteins: dynamin-like GTPases with antiviral activity. *Traffic* **3,** 710–717 CrossRef Medline
33. Lee, S. H., and Vidal, S. M. (2002) Functional diversity of Mx proteins: variations on a theme of host resistance to infection. *Genome Res.* **12,** 527–530 CrossRef Medline
34. Gao, S., von der Malsburg, A., Paeschke, S., Behlke, J., Haller, O., Kochs, G., and Daumke, O. (2010) Structural basis of oligomerization in the stalk region of dynamin-like MxA. *Nature* **465,** 502–506 CrossRef Medline
35. Schulte, B., Buffone, C., Opp, S., Di Nunzio, F., De Souza Aranha Vieira, D. A., Brandariz-Nuñez, A., and Diaz-Griffero, F. (2015) Restriction of HIV-1 requires the N-terminal region of MxB as a capsid-binding motif but not as a nuclear localization signal. *J. Virol.* **89,** 8599–8610 CrossRef Medline
36. Goujon, C., Greenbury, R. A., Papaioannou, S., Doyle, T., and Malim, M. H. (2015) A triple-arginine motif in the amino-terminal domain and oligomerization are required for HIV-1 inhibition by human MX2. *J. Virol.* **89,** 4676–4680 CrossRef Medline
37. Melén, K., Keskinen, P., Ronni, T., Sareneva, T., Lounatmaa, K., and Julkunen, I. (1996) Human MxB protein, an interferon-α-inducible GTPase, contains a nuclear targeting signal and is localized in the heterochromatin region beneath the nuclear envelope. *J. Biol. Chem.* **271,** 23478–23486 CrossRef Medline
38. Fricke, T., White, T. E., Schulte, B., de Souza Aranha Vieira, D. A., Dharan, A., Campbell, E. M., Brandariz-Nuñez, A., and Diaz-Griffero, F. (2014) MxB binds to the HIV-1 core and prevents the uncoating process of HIV-1. *Retrovirology* **11,** 68 CrossRef Medline
39. Dicks, M. D. J., Betancor, G., Jimenez-Guardeño, J. M., Pessel-Vivares, L., Apolonia, L., Goujon, C., and Malim, M. H. (2018) Multiple components of the nuclear pore complex interact with the amino-terminus of MX2 to facilitate HIV-1 restriction. *PLoS Pathog.* **14,** e1007408 CrossRef Medline
40. Kane, M., Rebensburg, S. V., Takata, M. A., Zang, T. M., Yamashita, M., Kvaratskhelia, M., and Bieniasz, P. D. (2018) Nuclear pore heterogeneity influences HIV-1 infection and the antiviral activity of MX2. *Elife* **7,** e35738 CrossRef Medline
41. Buffone, C., Schulte, B., Opp, S., and Diaz-Griffero, F. (2015) Contribution of MxB oligomerization to HIV-1 capsid binding and restriction. *J. Virol.* **89,** 3285–3294 CrossRef Medline
42. Dicks, M. D., Goujon, C., Pollpeter, D., Betancor, G., Apolonia, L., Bergeron, J. R., and Malim, M. H. (2016) Oligomerization requirements for MX2-mediated suppression of HIV-1 infection. *J. Virol.* **90,** 22–32 CrossRef Medline
43. Alvarez, F. J. D., He, S., Perilla, J. R., Jang, S., Schulten, K., Engelman, A. N., Scheres, S. H. W., and Zhang, P. (2017) CryoEM structure of MxB reveals a novel oligomerization interface critical for HIV restriction. *Sci. Adv.* **3,** e1701264 CrossRef Medline
44. Fribourgh, J. L., Nguyen, H. C., Matreyek, K. A., Alvarez, F. J. D., Summers, B. J., Dewdney, T. G., Aiken, C., Zhang, P., Engelman, A., and Xiong, Y.

(2014) Structural insight into HIV-1 restriction by MxB. *Cell Host Microbe* **16,** 627–638 CrossRef Medline

45. Goujon, C., Moncorgé, O., Bauby, H., Doyle, T., Barclay, W. S., and Malim, M. H. (2014) Transfer of the amino-terminal nuclear envelope targeting domain of human MX2 converts MX1 into an HIV-1 resistance factor. *J. Virol.* **88,** 9017–9026 CrossRef Medline
46. Busnadiego, I., Kane, M., Rihn, S. J., Preugschas, H. F., Hughes, J., Blanco-Melo, D., Strouvelle, V. P., Zang, T. M., Willett, B. J., Boutell, C., Bieniasz, P. D., and Wilson, S. J. (2014) Host and viral determinants of Mx2 antiretroviral activity. *J. Virol.* **88,** 7738–7752 CrossRef Medline
47. Matreyek, K. A., Wang, W., Serrao, E., Singh, P. K., Levin, H. L., and Engelman, A. (2014) Host and viral determinants for MxB restriction of HIV-1 infection. *Retrovirology* **11,** 90 CrossRef Medline
48. Li, J., Xu, F., Hu, S., Zhou, J., Mei, S., Zhao, X., Cen, S., Jin, Q., Liang, C., and Guo, F. (2015) Characterization of the interactions between SIVrcm Vpx and red-capped mangabey SAMHD1. *Biochem. J.* **468,** 303–313 CrossRef Medline
49. Shah, V. B., and Aiken, C. (2011) *In vitro* uncoating of HIV-1 cores. *J. Vis. Exp.* **8,** 3384 CrossRef Medline
50. Wei, W., Guo, H., Ma, M., Markham, R., and Yu, X. F. (2016) Accumulation of MxB/Mx2-resistant HIV-1 capsid variants during expansion of the HIV-1 epidemic in human populations. *EBioMedicine* **8,** 230–236 CrossRef Medline
51. Xu, D., Marquis, K., Pei, J., Fu, S. C., Cağatay, T., Grishin, N. V., and Chook, Y. M. (2015) LocNES: a computational tool for locating classical NESs in CRM1 cargo proteins. *Bioinformatics* **31,** 1357–1365 CrossRef Medline